Neuropsychologia 75 (2015) 50–60

Contents lists available at ScienceDirect

Neuropsychologia

journal homepage: www.elsevier.com/locate/neuropsychologia

Functional brain networks involved in reality monitoring

Paul D. Metzak [a,b], Katie M. Lavigne [a,b], Todd S. Woodward [a,b,*]

[a] Department of Psychiatry, University of British Columbia, Vancouver, Canada
[b] BC Mental Health and Addiction Research Institute, Vancouver, Canada

ARTICLE INFO

Article history:
Received 30 September 2014
Received in revised form
16 May 2015
Accepted 20 May 2015
Available online 21 May 2015

Keywords:
Source monitoring
Reality monitoring
Default-mode network
Functional connectivity
FMRI
PCA

ABSTRACT

Source monitoring refers to the recollection of variables that specify the context and conditions in which a memory episode was encoded. This process involves using the qualitative and quantitative features of a memory trace to distinguish its source. One specific class of source monitoring is reality monitoring, which involves distinguishing internally generated from externally generated information, that is, memories of imagined events from real events. The purpose of the present study was to identify functional brain networks that underlie reality monitoring, using an alternative type of source monitoring as a control condition. On the basis of previous studies on self-referential thinking, it was expected that a medial prefrontal cortex (mPFC) based network would be more active during reality monitoring than the control condition, due to the requirement to focus on a comparison of internal (self) and external (other) source information. Two functional brain networks emerged from this analysis, one reflecting increasing task-related activity, and one reflecting decreasing task-related activity. The second network was mPFC based, and was characterized by task-related deactivations in areas resembling the default-mode network; namely, the mPFC, middle temporal gyri, lateral parietal regions, and the precuneus, and these deactivations were diminished during reality monitoring relative to source monitoring, resulting in higher activity during reality monitoring. This result supports previous research suggesting that self-referential thinking involves the mPFC, but extends this to a network-level interpretation of reality monitoring.

1. Functional brain networks involved in reality monitoring

Source monitoring refers to the ability to distinguish the wide range of variables that specify the context and conditions in which a memory episode was encoded (Johnson et al., 1993). These conditions can include the sensory modality through which the memory was encoded, the media or agent through which the information was presented, the social, spatial, temporal, or affective context of the memory, or any other features which can serve to distinguish the origin of a memory. Although the source monitoring framework is very general, its core thesis is that memories are not inherently labeled as resulting from a particular source, but rather that the source information is retrievable on the basis of the qualitative and quantitative characteristics of the memories themselves (Lindsay and Byrne, 2008). Thus source monitoring involves both the memory of a particular episode, and a judgment process whereby the characteristics of that memory are interpreted and evaluated. For instance, it is likely that remembering a story one heard on the radio would be associated with a great deal of auditory information but little visual information or conceptual elaboration, which would help to correctly identify its modality and/or media source. While most source judgments are made quickly and automatically, the decision making process involved in distinguishing sources can also be slow and deliberative. These instances of strategic source monitoring usually involve both the recollection of perceptual details as well as the reasoning processes regarding the likelihood of the memory arising from different sources.

Accurate recollection of the sources of our memories has been an important research domain with regard to recovered memories (Geraerts et al., 2007; Raymaekers et al., 2012; Schacter et al., 1996; Stern and Rotello, 2000) and eyewitness testimony (Buratti et al., 2014; Leippe et al., 2009; Lindsay and Johnson, 1989; Lindsay, 1990; Loftus et al., 1978; Odinot et al., 2009) due to the serious consequences of memory distortions in these instances. A prominent aspect of source monitoring has been referred to as reality monitoring, which was originally proposed as the process of discriminating between external perceptual events, and internal thoughts and imaginings (Brandt et al., 2013; Johnson et al., 1988; Johnson et al., 1994; Johnson and Raye, 1981). Reality monitoring memories are distinguishable on the basis of their contents; for

* Corresponding author at: Room A3-A116, BC Mental Health & Addictions Research Institute–Translational Research Building, 3rd Floor, 938 W. 28th Avenue, Vancouver, British Columbia, Canada V5Z 4H4. Fax: +1 604 875 3871.
E-mail address: Todd.S.Woodward@gmail.com (T.S. Woodward).

http://dx.doi.org/10.1016/j.neuropsychologia.2015.05.014
0028-3932/

instance, one would expect that memories of external events would have more temporal, spatial, and sensory detail than events that were thought or imagined. They are also likely to contain more specific information than imagined events (Johnson and Raye, 1981). In contrast, memories formed solely from thought or imagination are likely to contain more traces of effortful cognitive operations, because imagining and thinking require more effort than mere perception (Hasher and Zacks, 1979).

Although a number of functional magnetic resonance imaging (fMRI) studies of source monitoring have reported that regions of the medial temporal lobes (MTL), parietal cortices, and prefrontal cortices are often preferentially activated (Dobbins et al., 2004; King and Miller, 2014; Mitchell et al., 2004; Mitchell and Johnson, 2009; Rugg et al., 1999; Wagner et al., 2005; Yonelinas, 2002), the medial prefrontal cortex (mPFC) has been shown to be active when making inferences about the mental states of other people (Frith and Frith, 2003), distinguishing between imagined and perceived events (Vinogradov et al., 2008), and the evaluation of internally generated information (Christoff et al., 2003), all of which support the idea that this region is involved in self-referential thinking (Araujo et al., 2013). Therefore, this region was of primary interest for the present study of self-other reality monitoring.

Task-related activity in any given brain area likely reflects the contributions of multiple brain networks (Friston, 2011). Studies on the neural basis of recollection have established that there are networks of regions which are typically found to be active during this mnemonic operation (Fornito et al., 2012; Rugg and Vilberg, 2013), which include regions of the default mode network (DMN) (Fox et al., 2005; Greicius et al., 2003; Raichle et al., 2001), and this network is thought to play a role in the processing of contextual associations (Bar, 2007). One of the core regions of the DMN is the mPFC (also known as fronto-polar cortex, rostral prefrontal cortex, ventromedial prefrontal cortex, or anterior prefrontal cortex). Combined with the involvement of the mPFC in self-referential thinking, this suggests that the study of the DMN may be important for understanding reality monitoring. Univariate task-based regression methods cannot separate activity of networks, but instead limit observations to the spatial and temporal effects combined over these networks (Braunlich et al., 2014); therefore, in the current study, we used a multivariate analysis method, constrained principal component analysis for fMRI (fMRI-CPCA) (Lavigne et al., 2015; Metzak et al., 2011, 2012), to study network-based involvement of the mPFC in realty monitoring.

In order to develop an appropriate control condition for reality monitoring, the generation effect (Slamecka and Graf, 1978) must be taken into account, which suggests that self-generated information is better recalled than other-generated information. Therefore, self-other reality monitoring experiments necessarily involve an intrinsic imbalance between the two retrieval conditions, such that one is more difficult than the other. An appropriate comparison condition for self-other reality monitoring requires not only another type of source monitoring, but also a parallel difficulty imbalance. In order to meet these requirements, we used recollection of which of two tasks was carried out on a given word: generation of a semantic associate (easier to recall) and reading (more difficult to recall). We hypothesized that reality monitoring, as a highly self-referential cognitive operation, would induce greater activity in an mPFC-based network (viz., the DMN) relative to a source monitoring control condition that did not involve self-other source recall.

2. Method

2.1. Participants

The participants were 30 healthy, English speaking volunteers (17 women and 13 men, mean age = 27.13 years, SD = 6.06). Participants were recruited via advertisements and word-of-mouth from the community of Vancouver, British Columbia, and participated in exchange for $10 per hour plus a copy of their structural brain images. All participants gave informed written consent prior to their participation.

2.2. Task design

For this study, the conditions of interest were Reality Monitoring (RM) and Source Monitoring (SM). In order to enhance comparison of RM and SM, a difficulty imbalance was built into both, with RM condition involving Self (easier recall) and Other (more difficult recall) subconditions, and the SM comparison condition involving Association (easier recall) and Read (more difficult recall) subconditions.

2.3. Encoding (not scanned)

Prior to functional scanning, participants were shown 30 words in each of the four randomly presented subconditions (120 words total): Self (or Internal), Other (or External), Association, and Reading. In the RM task condition (Self and Other subconditions), a jumbled word puzzle was presented in conjunction with a clue about the meaning of the word, for example, “BERAZ” would appear on the screen with the clue “a striped grazing animal”. In the Self subcondition, participants were required to say the target word aloud once they had solved the puzzle. In the Other subcondition, a pre-recorded voice said the target word aloud as soon as the jumbled word and clue appeared on the screen. For the Self and Other subconditions, participants pressed a key on the keyboard to advance to the next trial, and this experimental design was based on a previous study from our lab (Woodward et al., 2007).

In the SM task condition (Association and Read subconditions), a correctly spelled target word was presented in the center of the screen. In the Association subcondition, two other words were presented in the lower left and lower right corners. The participants were to indicate, via key press, which of the two words they felt was a closer semantic associate to the target word. For each target word, a strongly associated word and a weakly associated word were presented, with the relations selected based on the Edinburgh Associative Thesaurus (Kiss et al., 1973). The target word and the two semantic associates remained on the screen until the participant made a response. At that point, the target word and the selected associate remained on the screen for three seconds before the inter-trial interval (ITI) began. In the Read subcondition, the target word was presented in the center of the screen along with the instructions “Please read silently”. Participants were asked to press a key on the keyboard to advance to the next trial once they had finished reading the target word. Silent reading was required to avoid any perceptual input that might lead to the use of inner/outer information as a recall cue in the SM control condition. Thus, for the RM and SM encoding runs, the trials were self-paced. The ITI was 500 ms, during which an asterisk appeared on the screen. All words used in the encoding run were concrete nouns, and 2 versions of the encoding run were designed with RM and SM words switched between versions. These versions were counterbalanced between participants to minimize any version-specific effects. Please see Fig. 1 for a visual depiction of the encoding tasks.

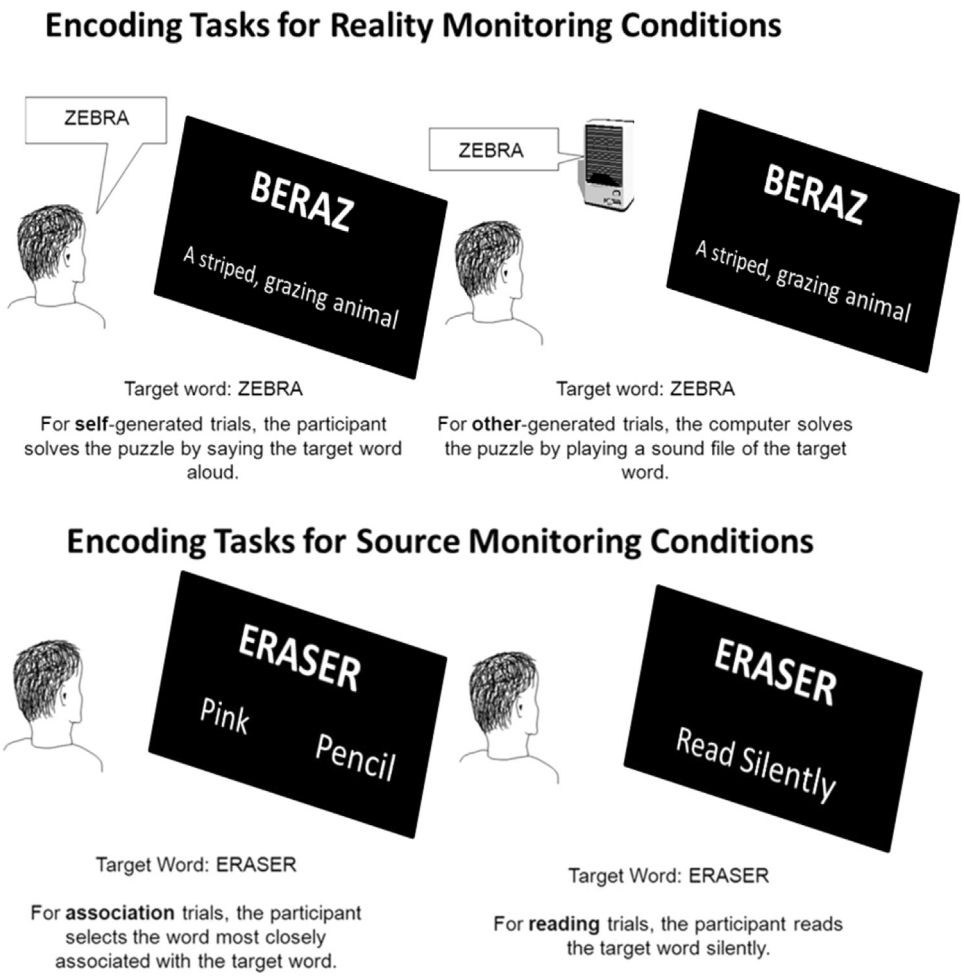

Fig. 1. Sample stimuli for the four conditions in the encoding portion of the experiment (not scanned).

2.4. Recollection (scanned)

After the completion of the encoding run, participants were taken to the MRI suite where they underwent a final MRI compatibility screening with the MRI technician prior to functional scanning. The recall run (scanned) began approximately 10 min after the encoding run (not scanned). All 120 words presented during the encoding run were presented during the recall run. The recall run lasted 15.5 min. Task switching research, including that from our lab (Allport et al., 1994; Jersild, 1927; Metzak et al., 2013; Rogers and Monsell, 1995; Woodward et al., 2008), has shown that when stimuli cue more than one instruction set, performance costs and the associated brain network activity are observable, and may obfuscate activity of the RM networks of interest for this study. Therefore, the stimuli were presented in RM and SM instruction blocks in order reduce the substantial cognitive load required to switch between instruction sets on a trial-by-trial basis (viz., self/other vs. associate/read response instructions).

Each RM block began with the following set of instructions printed on the screen: “Who solved it? You or Computer?”. Following this, twenty words from the Self and Other trials were presented sequentially in the center of the screen, and participants were asked to indicate, via key press, whether the puzzle was solved by “me” or the “computer”. The words “me” and “computer” appeared on the lower corners of the screen to remind participants of the response mapping. Participants used their index finger to select the option on the lower left corner of the screen, and their middle finger to select the option on the lower right corner of the screen. The side on which of “me” and “computer” appeared was alternated between participants.

Each SM block began with the following set of instructions being printed on the screen: “What did you do? Read silently or associate?” Then twenty words from the Associate and Read trials were presented sequentially in the center of the screen, and participants were asked to indicate, via key press, whether they had “associated” or “read” the target word. The words “associated” and “read” appeared on the lower corners of the screen to remind participants of the response mapping. Participants used their index finger to select the option on the lower left corner of the screen, and their middle finger to select the option on the lower right corner of the screen. The side on which “associated” and “read” appeared was alternated between participants.

Each block required 120 s to complete, and each target word was presented for a maximum of 5 s. The target word disappeared from the screen when a response was made, and the screen remained blank until the allotted 5 s for the trial elapsed. Each trial was separated with a 0, 1, or 2 s blank screen, followed by a 1 s interval where an asterisk was presented on the screen to warn the participants that the next trial was about to begin. A 10-s blank trial was inserted between each block for which the word “Relax” was presented for the first 9 s, followed by a blank screen for 1 s to alert the participant that the next block was beginning. Following this blank trial, the instructions for the block were presented on the screen for 3 s. Please see Fig. 2 for a depiction of the Recollection task. The jittered ITI, combined with the blank screen following response, the Relax screen, and the instruction screen,

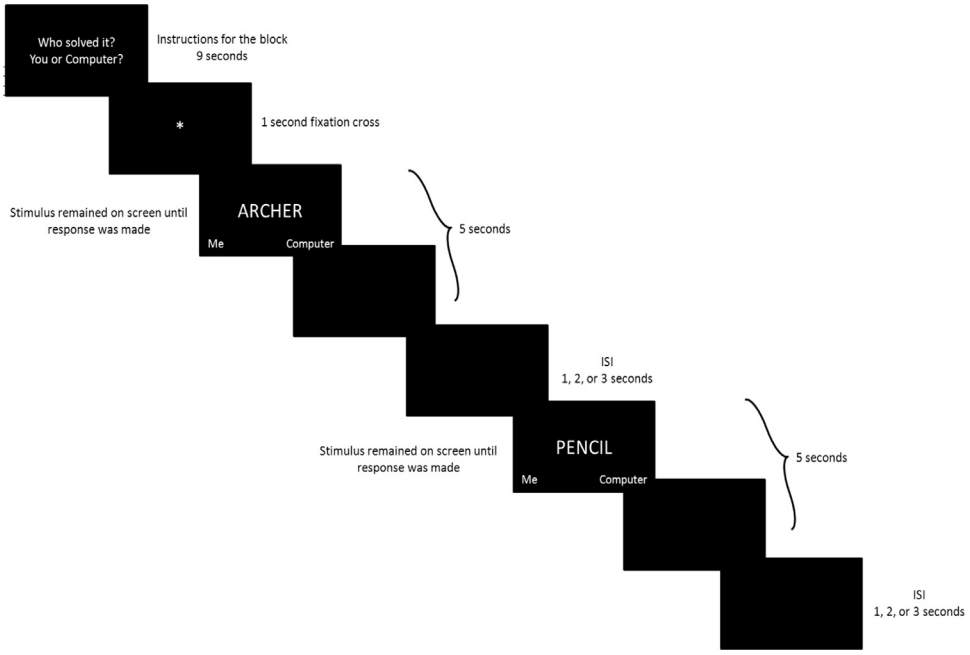

Fig. 2. Sample stimuli and timing for the recollection portion of the experiment (scanned).

provided a roughly logarithmic distribution of ITIs, optimizing efficiency of event-related analysis methods (Serences, 2004).

2.5. Image processing

Imaging was performed at the University of British Columbia's MRI Research Centre on a Phillips Achieva 3.0 T MRI scanner with Quasar Dual Gradients (maximum gradient amplitude 80 mT/m and a maximum slew rate of 200 mT/m/s). The participant's head was firmly secured using a custom head holder. Functional images volumes were collected using a T2*-weighted gradient echo spin pulse sequence (TR/TE=2000/30 ms, flip angle 90°, 36 slices, 3 mm thick, 1 mm gap, sense factor 2, 80×80 matrix reconstructed at 128, FOV 240.0 mm, measured voxel is 1.875 mm × 1.875 mm × 3.972 mm, actual band width=53.4 Hz per pixel) effectively covering the whole brain (145 mm axial extent). Functional images were reconstructed offline, and the scan series was realigned and normalized using the method implemented in Statistical Parametric Mapping 8 (SPM8; http:/www.fil.ion.ucl.ac.uk/spm). Translation and rotation corrections did not exceed 3 mm or 3° for any of the participants. Parameters for spatial normalization into the modified Montreal Neurological Institute (MNI) space used in SPM8 were determined using the echo planar imaging (EPI) template provided by SPM8 and the mean functional images constructed from the realigned images of each participant and scan series. Voxels were normalized to 3 mm × 3 mm × 3 mm. The normalized functional images were smoothed with an 8 mm full width at half maximum Gaussian filter.

2.6. Neuroimaging data analysis procedure

The neuroimaging data were analyzed using the Constrained Principal Component Analysis for fMRI software package (fMRI-CPCA; www.nitrc.org/projects/fmricpca). Only data from correct trials were submitted to the fMRI-CPCA analysis.

The details of the fMRI-CPCA method are presented elsewhere (Metzak et al., 2011, 2012; Woodward et al., 2013; Woodward et al., 2006). For the comprehensive CPCA theory and proofs please see previously published work (Hunter and Takane, 2002; Takane and Hunter, 2001; Takane and Shibayama, 1991). Briefly, after variance in the blood oxygenation level dependent (BOLD) signal predictable from task timing has been separated from that not predicable from task timing, the dominant patterns of inter-correlation between voxels over time were used to derive functional networks. The use of a finite impulse response (FIR) model allowed a hemodynamic response (HDR) shape to be estimated for each functional network identified.

We now briefly present matrix equations for the current application of CPCA. This application of CPCA involved the preparation of two matrices. The first matrix, *Z*, contained the BOLD time series of each voxel, with one column per voxel and one row per scan. Each column contained realigned, normalized and smoothed activations over all scans, carried out for each subject separately. The second matrix, *G*, contained the FIR models of the expected BOLD response to the timing of stimulus presentations.

2.7. Preparation of G

The *G* (design) matrix consisted of a FIR basis set, which can be used to estimate the increase in BOLD signal at specific post-stimulus scans relative to all other scans. The value 1 was placed in rows of *G* for which BOLD signal amplitude was to be estimated, and the value 0 in all other rows ("mini boxcar" functions). The time points for which a basis function was specified in the current study were the 1st to 10th scans following stimulus presentation, resulting in an event-related analysis method. This allowed removal of incorrect trials from the analysis. Since the repetition time (TR) for these data was 2 s, this resulted in estimating BOLD signal over a 20 s window, with the start of the first time point (time=0) corresponding to encoding stimulus onset. In this analysis we created a *G* matrix that would allow us to estimate subject-and-condition specific effects by inserting a separate FIR basis set for each task and difficulty condition and for each individual subject. The columns in this subject-and-condition based *G* matrix code 10 poststimulus time points, 2 task conditions (RM vs. SM), 2 difficulty conditions (Easy to Recall vs. Hard to Recall), and 30 subjects, resulting in 1200 columns ($10 \times 2 \times 2 \times 30 = 1200$).

2.8. Matrix equations

The matrix of BOLD time series and design matrices are taken as input, with BOLD in Z being predicted from the FIR model in G. In order to achieve this, multivariate least-squares linear regression was carried out, whereby the BOLD time series (Z) was regressed onto the design matrix (G):

$$Z = GC + E, \quad (1)$$

where $C = (G'G)^{-1}G'Z$ using least squares regression. This analysis yielded condition-specific regression weights in the C matrix (i.e., regression weights specific to the experimental conditions as defined by the design matrix). The condition-specific regression weights are often referred to (in conventional fMRI analyzes) as beta images. GC contains variability in Z that was predictable from the design matrix G, that is to say, variability in Z that was predictable from the timing of stimulus presentations. For the analysis presented here, the Z and G matrices were standardized for each subject separately.

The next step used singular value decomposition to extract components representing networks of functionally interconnected voxel activations from GC that were related to the experimental stimulus presentations. This involved singular value decomposition of the activation variability that was predictable from the design matrix (GC):

$$UDV' = GC, \quad (2)$$

where U=matrix of left singular vectors; D=diagonal matrix of singular values; V=matrix of right singular vectors. Each column of $VD/\sqrt{(m-1)}$, where m=the number of rows in Z, was overlaid on a structural brain image to allow visualization of the neural regions involved in each functional network. In the current application of CPCA, we orthogonally rotated (Metzak et al., 2011) and rescaled the VD matrix prior to display, so that a rotated *loading matrix* is displayed. The values of the loading matrix contain the correlations between the components in U and the variables in GC. An orthonormal rotation transformation matrix was then used to transform the rescaled left singular vectors U into rotated component scores (with rows corresponding to scans).

2.9. Predictor weights

To interpret the components with respect to the conditions represented in G, we produced *predictor weights* (Hunter and Takane, 2002) in matrix P. These weights were applied to each column of the matrix of predictor variables (G) to create U ($U=GP$) and were orthogonally rotated by applying the same transformation matrix (Metzak et al., 2011) as was applied to VD and U. The values in P indicated the importance of each column in the G matrix to the network(s) represented by the component(s), so were essential for relating the resultant components to the experimental conditions of interest represented in G. This approach estimated an HDR shape for each individual separately, so it fully accommodated inter-subject heterogeneity. These were the values that are averaged over subjects and plotted to observe the HDR shape for each component.

2.10. Statistical tests of component reliability

As is explained above, predictor weights were produced for each combination of poststimulus time point, task condition, difficulty condition, and subject. These weights were used to statistically test the effect of poststimulus time, and plotted to determine whether or not these values reflected a true HDR shape (and not simply varying randomly around zero). The impact of the experimental manipulation (viz., RM and SM) on the estimated HDR shapes was also tested statistically. This was reflected by a significant main effect of either Task or Difficulty, or an interaction between these factors and Time Point for the measure of estimated HDR (i.e., the predictor weights). This analysis was carried out as a $10 \times 2 \times 2$ within-subjects ANOVA for each component, with the factors of Time Point (time points 1–10 after the initiation of a task trial), Task (RM, or SM), and Difficulty (Easy to Recall, or Hard to Recall) as within-subject factors. Selecting "repeated" contrasts for the within-subjects factor of Task, Difficulty, and Time Point allowed complex interactions to be broken down into simpler 2×2 interactions between the factors at adjacent Time Points. Inspection of the comparative effect sizes associated with these 2×2 interactions were used to interpret the significant complex interactions. Tests of sphericity were carried out for all ANOVAs. Greenhouse–Geisser adjusted degrees of freedom for violations of sphericity were inspected but did not affect the results; therefore, the original degrees of freedom are reported. The orthogonally rotated and rescaled VD matrix was overlaid on structural brain images for depiction of the spatial arrangement of the functional networks.

3. Results

3.1. Behavioral results

For a summary of the behavioral results, please see Table 1. The response times (RT) were analyzed using a $2 \times 2 \times 2$ within subjects repeated-measures ANOVA with factors of Task (RM vs. SM), Difficulty (Easy to Recall vs. Difficult to Recall), and Performance (Correct vs. Incorrect). For the RT analysis, there were main effects of Task, $F(1,23)=9.43$, $p<.01$, $\eta^2=.29$, Difficulty, $F(1,23)=25.08$, $p<.001$, $\eta^2=.52$, and Performance, $F(1,23)=31.78$, $p<.001$, $\eta^2=.58$. These significant main effects were due to increased RTs in the Source Monitoring condition, the Difficult to Recall condition, and Incorrect responses, respectively. All interactions were non-significant (all $ps>.14$), which suggests that the difficulty imbalance, as measured by RT, was successfully matched between the RM and SM conditions.

The correct response counts were analyzed using a 2×2 within subjects repeated-measures ANOVA, with factors of Task (RM vs. SM) and Difficulty (Easy to Recall vs. Difficult to Recall). No main effects or interactions were significant for correct response counts (all $ps>.3$), suggesting that the difficulty imbalance in the SM and RM conditions was captured by RTs but not by correct response counts.

Table 1
Mean accuracy rates and response times in milliseconds. Standard errors are in parentheses.

	Source monitoring				Reality monitoring			
	Association		Read		Self		Other	
Accuracy	76.23% (4.70%)		72.10% (4.64%)		73.00% (4.51%)		75.77% (4.91%)	
	Correct	Incorrect	Correct	Incorrect	Correct	Incorrect	Correct	Incorrect
Response times	960.89 (43.38)	1260.80 (67.17)	1161.65 (40.54)	1371.67 (65.67)	883.22 (50.78)	1158.63 (58.06)	1066.58 (45.43)	1175.06 (62.04)

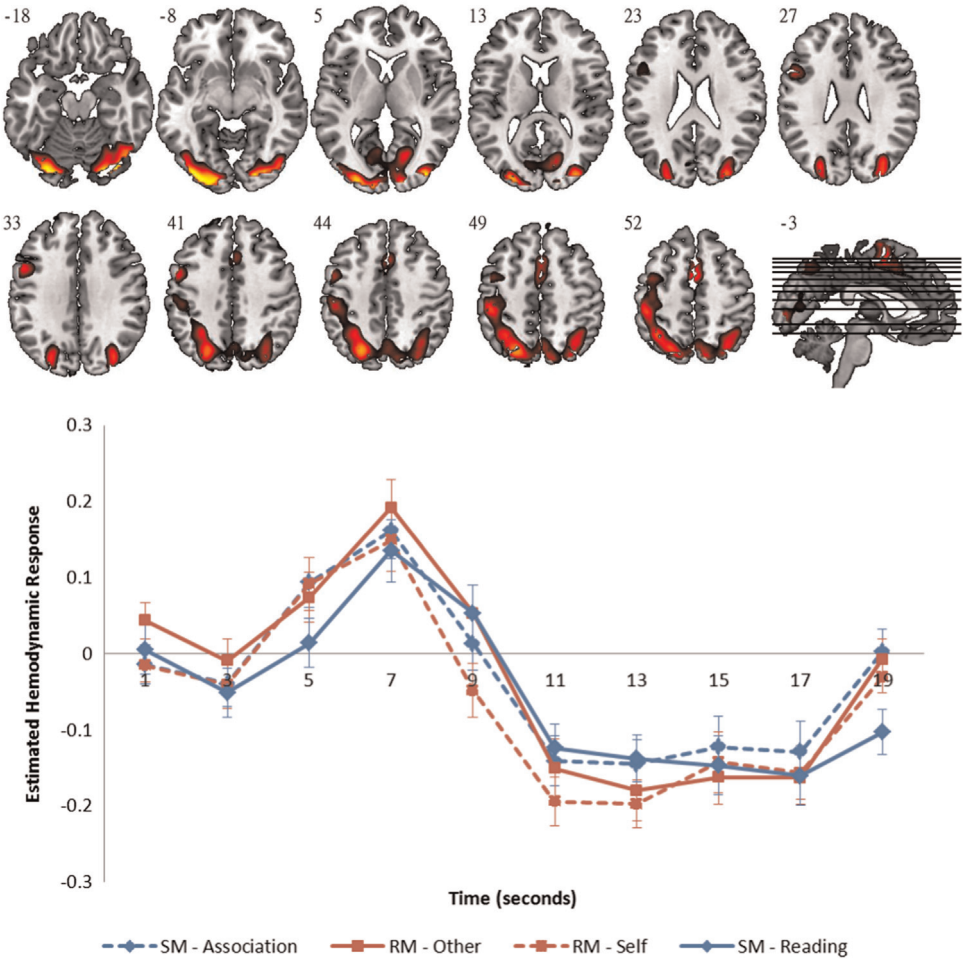

Fig. 3. The upper image depicts the dominant 10% of component loadings for Component 1. Positive loadings are depicted in red/yellow (min = 0.19, max = 0.29) and represent task-based increases in BOLD signal. No negative loadings exceeded the 10% threshold. Montreal Neurological Institute (MNI) *z*-axis coordinates are displayed. The lower image depicts the mean FIR-based predictor weights plotted as a function of poststimulus time. RM tasks are plotted in red (Other and Self subconditions), and SM tasks are plotted in blue (Association and Read subconditions). Easy to remember conditions are plotted with dashed lines, and difficult to remember conditions are plotted with solid lines. (For interpretation of the references to color in this figure legend, the reader is referred to the web version of this article.)

3.2. Neuroimaging results

An examination of the scree plot (Cattell, 1966) suggested that 2 components should be extracted for further significance testing. The sum of the squared loadings divided by the number of scans (analogous to the percentage of predictable variance accounted for by each component) for the rotated solution was 14.61 and 9.08 for components 1 and 2 respectively. The brain regions comprising the functional networks represented by each component (i.e., each row of the rotated and rescaled right singular vector *VD*), were thresholded to the top 10% of loadings, mapped onto an MNI structural image, and are displayed in Figs. 3 and 4 (upper panels), with corresponding anatomical descriptions in Tables 2 and 3. The mean predictor weights plotted as a function of poststimulus time, representing the estimated HDR of each functional network, are listed in Figs. 3 and 4 (lower panels). The repeated-measures ANOVAs of the predictor weights for each component resulted in significant interactions for both components. As mentioned above, the initial $10 \times 2 \times 2$ ANOVA was performed with the factors of Time Point, Task, and Difficulty, and significant interactions were interpreted by examining the effect sizes from the simpler 2×2 interactions involving adjacent time points. The set of univariate results from this experiment are reported in the Supplementary Material.

3.3. Component 1 (Task Positive)

Briefly, component 1 was comprised of bilateral activations in the visual cortices (Brodmann's Areas (BAs) 17, 18, 19), cerebellum, supplementary motor area (SMA; BA 6), anterior cingulate gyrus (BA 24), and superior parietal regions (BA 40). These activations also extend into the left pre-and post-central gyri (BAs 6 and 2, respectively). This pattern of brain activity is found near universally when performing cognitively demanding tasks including recollection (Fornito et al., 2012), and has been referred to as the task positive network (Fox et al., 2005), the multiple demands network (Duncan and Owen, 2000), or the dorsal attention network (Corbetta et al., 2008; Corbetta and Shulman, 2002).

For this component, the Task × Time Point interaction (i.e., the effect of experimental interest) was not significant, $F(9,252) = 0.60$, $p > .50$, $\eta^2 = .02$. The ANOVA revealed a significant Difficulty × Time Point interaction, $F(9,252) = 2.39$, $p < .05$, $\eta^2 = .08$. The follow up inspection of 2×2 interactions of adjacent levels of the Time Points factor showed that the strongest Difficulty effects occurred between 3 and 5 seconds poststimulus time ($\eta^2 = .17$), 5 and 7 s poststimulus time ($\eta^2 = .16$), and 6 and 8 s poststimulus time ($\eta^2 = .20$), with all other effect sizes of adjacent levels of the Time Point factor producing smaller effect sizes ($\eta^2 = .07$ or lower). Inspection of the predictor weight graphs in Fig. 3 indicate that this significant interaction was due to the HDRs for the difficult-to-

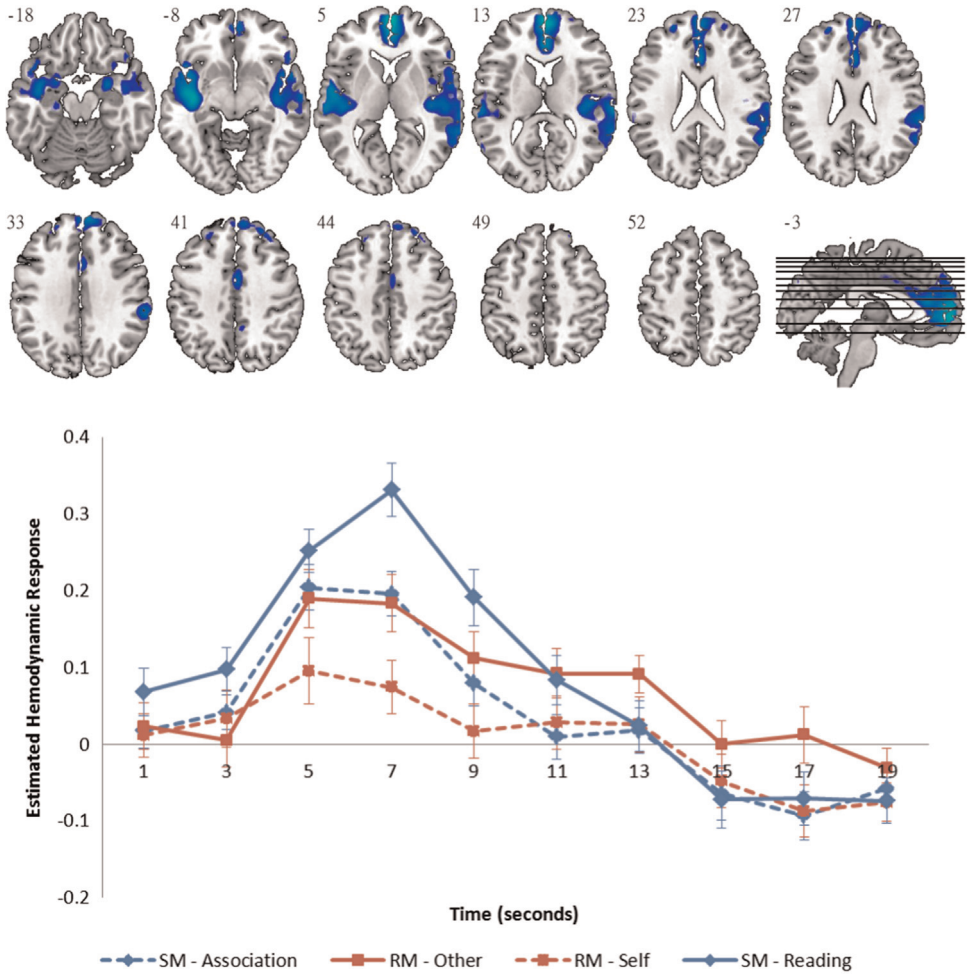

Fig. 4. The upper image depicts the dominant 10% of component loadings for Component 2. Negative loadings are depicted in blue/green (min= −0.15, max= −0.23), and represent task-based reductions in BOLD signal. No positive loadings exceeded the 10% threshold. Montreal Neurological Institute (MNI) *z*-axis coordinates are displayed. The lower image depicts the mean FIR-based predictor weights plotted as a function of poststimulus time. RM tasks are plotted in red (Other and Self subconditions), and SM tasks are plotted in blue (Association and Read subconditions). Easy to remember conditions are plotted with dashed lines, and difficult to remember conditions are plotted with solid lines. (For interpretation of the references to color in this figure legend, the reader is referred to the web version of this article.)

recall subconditions (Reading and Other) displaying a sharper slope to the peak, and a delayed reduction in activity to baseline relative to the easier-to-recall subconditions (Association and Self).

3.4. Component 2 (Default Mode)

Component 2 was comprised of bilateral deactivations in the mPFC (BA 10), middle and superior temporal gyri (BAs 21, 22, 38, 41, 42), lateral parietal regions (BAs 39, 40), and the precuneus (BA 23). Similar patterns of deactivity are essentially ubiquitous when performing effortful cognitive tasks, and has been termed the DMN (or task negative network) (Greicius et al., 2003; Raichle et al., 2001; Vincent et al., 2006).

The ANOVA revealed a significant Task × Time Point interaction (i.e., the effect of experimental interest), $F(9,252)=4.10$, $p<.01$, $\eta^2=.13$. The follow up inspection of 2 × 2 interactions of adjacent Time Points showed that the largest differences in HDR between the RM and SM conditions occurred between 7 and 9 s poststimulus time ($\eta^2=.16$), and 9 and 11 s poststimulus time ($\eta^2=.31$), with all other effect sizes of adjacent levels of the Time Point factor producing smaller effect sizes ($\eta^2=.12$ or lower). Inspection of the predictor weights indicated that these significant differences were due to stronger deactivations in the SM conditions relative to the RM conditions.

A significant Difficulty × Time Point interaction was also present, $F(9,252)=4.68$, $p<.001$, $\eta^2=.14$. The follow up inspection of 2 × 2 interactions of adjacent Time Points revealed that the largest differences in HDR between the Difficulty conditions occurred between 3 and 5 s poststimulus time, $\eta^2=.13$, and 5 and 7 s poststimulus time, $\eta^2=.16$, with all other effect sizes of adjacent levels of the Time Point factor producing smaller effect sizes ($\eta^2=.11$ or lower). Inspection of the predictor weights in Fig. 4 indicate that these significant differences are due to stronger deactivations in the difficult-to-recall subconditions (Reading and Other) relative to the easier-to-recall subconditions (Association and Self).

4. Discussion

The purpose of the present study was to identify functional brain networks that underlie reality monitoring, using an alternative type of source monitoring as a control condition. On the basis of previous studies on self-referential thinking, it was expected that a mPFC-based network would be more active during reality monitoring than the control condition, due to the requirement to focus on a comparison of internal (self) and external (other) source information. Two functional brain networks emerged from this analysis, one reflecting increasing task-related activity, and one reflecting decreasing task-related activity (DMN).

Table 2
Cluster volumes for top 10% of loadings found in Component 1, with anatomical descriptions, Montreal Neurological Institute (MNI) coordinates, and Brodmann Areas (BAs) for peaks within each cluster. Only positive loadings are reported as no negative loadings appeared in the top 10% of loadings for Component 1. Clusters smaller than 270 mm^3 were omitted.

Cortical regions	Cluster volume		BAs for peak location	MNI coordinate for peak location		
	Voxels	(mm^3)		*x*	*y*	*z*
Cluster 1: Bilateral	4865	131,355				
Occipital fusiform gyrus			18	27	−85	−14
Inferior lateral occipital cortex			19	36	−82	−14
Inferior lateral occipital cortex			19	−39	−88	−8
Occipital fusiform gyrus			18	−30	−85	−17
Occipital pole			19	−33	−91	−5
Superior lateral occipital cortex			7	−24	−70	46
Superior lateral occipital cortex			19	30	−88	22
Occipital pole			18	15	−91	−2
Superior parietal lobule			40	−36	−55	55
Postcentral gyrus			2	−45	−34	52
Precentral gyrus			6	−36	−10	61
Intracalcarine cortex			18	15	−73	7
Cerebellum (Lobule VI)			N/A	33	−55	−26
Precuneus			7	3	−67	49
Intracalcarine cortex			18	−15	−76	7
Lingual gyrus			17	−9	−64	4
Cerebellum (Crus II)			N/A	6	−79	−29
Precuneus			7	−3	−55	64
Cluster 2: Bilateral	345	9315				
Supplementary motor area			6	0	2	58
Paracingulate gyrus			32	0	14	49
Cluster 3: Left hemisphere						
Cerebellum (Crus VI)			N/A	−36	−52	−23

The DMN was mPFC based, and was characterized by task related deactivations in the mPFC, middle and superior temporal gyri, lateral parietal regions, and the precuneus. The DMN deactivation was diminished during reality monitoring relative to source monitoring, resulting in higher activity during reality monitoring relative to source monitoring. This result supports previous research suggesting that self-referential thinking involves the mPFC, but extends this to a network-level interpretation of RM.

The pattern of deactivity seen in the mPFC-based component was characterized by deactivations relative to baseline in the mPFC, middle and superior temporal gyri, lateral parietal regions, and the precuneus, generally matching the configuration of the DMN (Greicius et al., 2003; Raichle et al., 2001; Vincent et al., 2006). Relating the dominant regions of Component 2 to the recently proposed 7-network brain parcellation derived from resting state data (Buckner et al., 2011; Choi et al., 2012; Yeo et al., 2011), mPFC and posterior supramarginal gyrus/posterior middle temporal gyrus deactivations were located on the DMN, but superior temporal deactivations (including primary auditory cortices) were located on the Ventral Attention and Somatosensory networks. The interaction between Task and Time Point was attributable to the increase in deactivity in the SM relative to RM; in other words, this component serves to demarcate a difference between RM and SM, with this difference being due to weaker deactivation of the mPFC-based DMN in the RM condition. We interpreted this reduction in deactivity in the RM condition as being related to self-referential thinking in the RM condition, as previous research has shown that the mPFC is activated by these types of tasks, including autobiographical planning (Araujo et al., 2013; Spreng, 2012) and theory of mind (Gallagher and Frith, 2003; Mar, 2011). In the current study, as in many of the instances reported in the previous literature, this 'activation' of the mPFC is due to less deactivation in reality monitoring conditions, rather than activation proper (Brandt et al., 2013; Cansino, 2002; Kensinger and Schacter, 2006; Simons et al., 2005; Subramaniam et al., 2012; Vinogradov et al., 2006). The auditory cortex deactivation involvement on the mPFC-based DMN was not hypothesized. However, similar patterns of auditory cortex deactivity have been found in studies specifically examining the effects of cross-modal stimuli on sensory cortices (Laurienti et al., 2002), and in memory experiments employing visual encoding (Lavigne et al., 2015; Metzak et al., 2011, 2012; Woodward et al., 2013). It is also possible that auditory cortex may be found on this network due to the auditory features of the RM stimuli that were encoded prior to entering the scanner. The greater deactivation in this component in the difficult to remember conditions (Reading and Other) has also been found in previous literature examining the DMN (McKiernan et al., 2003; Metzak et al., 2011, 2012) and may reflect reductions in spontaneous thoughts under attentionally demanding task conditions.

The component with activity increasing relative to baseline (Component 1) displayed the strongest activations in visual cortex, cerebellum, SMA, anterior cingulate, and left pre- and post-central gyri. This pattern of brain activity is found near universally when performing cognitively demanding tasks including recollection (Fornito et al., 2012), and similar patterns have been referred to as the task positive network (TPN; Fox et al., 2005), the multiple demands network (Duncan and Owen, 2000), the dorsal attention network (Corbetta et al., 2008; Corbetta and Shulman, 2002), or the frontoparietal network (Yeo et al., 2011). Relating the TPN to the recently proposed 7-network brain parcellation derived from resting state data (Buckner et al., 2011; Choi et al., 2012; Yeo et al., 2011), the dACC activity was located on the Ventral Attention Network, the occipital activation on the Visual Network, and the lateral frontal, superior partial and cerebellar activations on the Dorsal Attention Network.

We found that the estimated HDRs from this component revealed an interaction between Difficulty and Time. All conditions peaked at 6 s poststimulus time, however, the easier to recall tasks (Association and Self stimuli) increased in activity more quickly and returned to baseline earlier than the more difficult to recall tasks (Reading and Other stimuli). Difficulty-related modulations in this network have been found previously in working memory studies (Metzak et al., 2011, 2012) as well as in a study using a visuospatial paired associates learning task (Gould et al., 2003). The slower rise to peak and return to baseline of the estimated HDRs in the Difficult conditions in this component is mirrored by the significant differences in RT between the Easy and Difficult conditions, and is assumed to reflect differences in task demands and requirements for attentional resources (although see Grinband et al., 2011 for an alternative explanation). These results suggest that this network is not specifically related either to source or reality monitoring, as opposed to the pattern of activity found in the DMN component, but rather plays a general role in the recollection of these types of stimuli and may reflect differences in recall difficulty (Duncan and Owen, 2000). This interpretation is supported by a recent review of brain networks underlying recollection, which identified qualitatively similar networks as being active during this process (Fornito et al., 2012). Our results support the interpretation that interactions between the DMN and TPN are generally competitive but that they can work somewhat cooperatively as well, as in the present study the anticorrelation

Table 3
Cluster volumes for top 10% of loadings found in Component 2, with anatomical descriptions, Montreal Neurological Institute (MNI) coordinates, and Brodmann Areas (BAs) for peaks within each cluster. Only negative loadings are reported as no positive loadings appeared in the top 10% of loadings for Component 2. Clusters smaller than 270 mm^3 were omitted.

Cortical regions	Cluster volume		BAs for peak location	MNI coordinate for peak location		
	Voxels	(mm^3)		*x*	*y*	*z*
Cluster 1: Right hemisphere	2291	61,857				
Planum Temporale			22	66	−22	16
Supramarginal gyrus			40	63	−34	28
Anterior superior temporal gyrus			21	60	2	−2
Amygdala			N/A	24	−1	−20
Angular gyrus			40	63	−49	19
Temporal pole			38	54	11	−8
Planum polare			N/A	39	−19	−2
Posterior middle temporal gyrus			22	63	−46	7
Transverse temporal gyrus			42	42	−19	10
Posterior superior temporal gyrus			21	63	−10	−8
Parietal operculum cortex			41	48	−31	19
Inferior Frontal Gyrus (pars traingularis)			45	54	26	−2
Anterior middle temporal gyrus			20	48	−1	−26
Anterior parahippocampal gyrus			36	30	5	−29
Orbitofrontal cortex			47	33	20	−20
Inferior lateral occipital cortex			39	57	−67	16
Cluster 2: Bilateral	1472	39,744				
Frontal pole			10	0	59	4
Anterior cingulate gyrus			24	0	38	13
Middle cingulate gyrus			24	3	−1	40
Superior frontal gyrus			9	−3	47	49
Cluster 3: Left hemisphere	1330	35,910				
Insula			N/A	−39	−13	−8
Temporal pole			38	−48	11	−11
Planum temporale			22	−63	−25	7
Anterior parahippocampal gyrus			34	−24	2	−20
Superior lateral occipital cortex			37	−60	−61	16
Posterior supramarginal gyrus			42	−63	−46	22
Anterior middle temporal gyrus			21	−57	−7	−20
Cluster 4: Left hemisphere	99	2673				
Middle Frontal gyrus			46	−24	53	28
Cluster 5: Right hemisphere	33	891				
Inferior Frontal gyrus (pars orbitalis)			47	45	44	−5
Cluster 6: Bilateral	21	567				
Cuneus			18	3	−85	34
Cluster 7: Bilateral	14	378				
Precuneus			23	6	−46	40

between these two networks was reduced in the RM condition.

There are several limitations of this study. First, other differences between the control and experimental conditions may have contributed to the results, some due to state effects associated with block designs. For example, in the RM condition, participants were shown scrambled words whereas in the SM condition, the stimulus words were unscrambled. Furthermore, as mentioned above, the Self and Other subconditions involved encoding a spoken word, whereas the encoding in the SM subconditions were purely visual, raising the possibility that the superior temporal increase in RM was due to this confound. However, the network activity was reduced in the Other condition relative to the Self condition, which aligns with the hypothesized-network interpretation rather than the auditory confound interpretation, since the confound interpretation would predict the greater or equal primary auditory cortex increase in the Other subcondition. This issue remains an open topic of investigation for future network based studies of reality monitoring which could be resolved by developing a SM control condition that uses auditory stimuli.

Second, the encoding portion of this experiment was not scanned, and may be an important extension to the current study, as it would allow a clarification of the relations between brain network activity during encoding and subsequent recall. Third, although we did see the predicted effect of a difficulty imbalance in the RTs, there was no evidence of a difficulty imbalance in the accuracy rates for the behavioral results. This may indicate that RT is a more sensitive measure for detecting this difficulty imbalance but this interpretation requires more rigorous testing. Finally, in this study only correct responses were analyzed, leaving the brain activity patterns underlying unsuccessful recall unexplored.

This study examined differences in functionally connected networks during the performance of SM and RM tasks. An mPFC-based DMN was characterized by a pattern of task-related deactivation which was diminished during reality monitoring relative to source monitoring, resulting in higher activity during reality monitoring relative to source monitoring. This result supports previous research suggesting that self-referential thinking involves the mPFC, but extends this to a network-level interpretation involving the DMN. This result has relevance to clinical research such as that involving schizophrenia and autism, as these disorders are characterized by inner/outer confusion (Allen et al., 2012; Lavigne et al., 2015; Woodward et al., 2007), and deficits in self-other matching (Williams, 2008).

Acknowledgments

This project was supported by a Scholar Award from the Michael Smith Foundation for Health Research (MSFHR) (Grant no.

CI-SCH-00073(05-1)), a New Investigator Award from the Canadian Institutes of Health (CIHR), and a CIHR operating grant (MOP-64431) to TSW; as well as Doctoral Research Awards for PDM and KML. The authors acknowledge the UBC High Field Magnetic Resonance Imaging Center, thank John Paiement for assistance with computer programming, and Tara Cairo for assistance with stimulus preparation.

Appendix A. Supplementary Information

Supplementary data associated with this article can be found in the online version at http://dx.doi.org/10.1016/j.neuropsychologia.2015.05.014.

References

Allen, P., Modinos, G., Hubl, D., Shields, G., Cachia, A., Jardri, R., Hoffman, R., 2012. Neuroimaging auditory hallucinations in schizophrenia: from neuroanatomy to neurochemistry and beyond. Schizophr. Bull. 38 (4), 695–703.
Allport, A., Styles, E., Hsieh, S., 1994. Shifting intentional set: Exploring the dynamic control of tasks, Attention and performance 15: Conscious and Nonconscious Information Processing. The MIT Press, Cambridge, MA US, pp. 421–452.
Araujo, H.F., Kaplan, J., Damasio, A., 2013. Cortical midline structures and autobiographical-self processes: an activation-likelihood estimation meta-analysis. Front. Hum. Neurosci. 7, 548.
Bar, M., 2007. The proactive brain: using analogies and associations to generate predictions. Trends Cognit. Sci. 11 (7), 280–289.
Brandt, V., Bergström, Z., Buda, M., Henson, R.A., Simons, J.S., 2013. Did I turn off the gas? Reality monitoring of everyday actions. Cognit., Affect., Behav. Neurosci., 1–11.
Braunlich, K., Gomez-Lavin, J., Seger, C.A., 2014. Frontoparietal networks involved in categorization and item working memory. NeuroImage.
Buckner, R.L., Krienen, F.M., Castellanos, A., Diaz, J.C., Yeo, B.T.T., 2011. The organization of the human cerebellum estimated by intrinsic functional connectivity. J. Neurophysiol. 106 (5), 2322–2345.
Buratti, S., Allwood, C.M., Johansson, M., 2014. Stability in the metamemory realism of eyewitness confidence judgments. Cognit. Process. 15 (1), 39–53.
Cansino, S., 2002. Brain activity underlying encoding and retrieval of source memory. Cerebr. Cortex 12 (10), 1048–1056.
Cattell, R.B., 1966. The scree test for the number of factors. Multivariate Behav. Res. 1 (2), 245–276.
Choi, E.Y., Yeo, B.T.T., Buckner, R.L., 2012. The organization of the human striatum estimated by intrinsic functional connectivity. J. Neurophysiol. 108 (8), 2242–2263.
Christoff, K., Ream, J.M., Geddes, L.P.T., Gabrieli, J.D.E., 2003. Evaluating self-generated information: anterior prefrontal contributions to human cognition. Behav. Neurosci. 117 (6), 1161–1168.
Corbetta, M., Patel, G., Shulman, G.L., 2008. The reorienting system of the human brain: from environment to theory of mind. Neuron 58 (3), 306–324.
Corbetta, M., Shulman, G.L., 2002. Control of goal-directed and stimulus-driven attention in the brain. Nat. Rev. Neurosci. 3 (3), 201–215.
Dobbins, I.G., Simons, J.S., Schacter, D.L., 2004. fMRI evidence for separable and lateralized prefrontal memory monitoring processes. J. Cognit. Neurosci. 16 (6), 908–920.
Duncan, J., Owen, A.M., 2000. Common regions of the human frontal lobe recruited by diverse cognitive demands. Trends Neurosci. 23 (10), 475–483.
Fornito, A., Harrison, B.J., Zalesky, A., Simons, J.S., 2012. Competitive and cooperative dynamics of large-scale brain functional networks supporting recollection. Proc. Natl. Acad. Sci. USA 109 (31), 12788–12793.
Fox, M.D., Snyder, A.Z., Vincent, J.L., Corbetta, M., Van Essen, D.C., Raichle, M.E., 2005. The human brain is intrinsically organized into dynamic, anticorrelated functional networks. Proceedings of the National Academy of Sciences of the United States of America 102 (27), 9673–9678.
Friston, K.J., 2011. Functional and effective connectivity: a review. Brain Connect *1* (1), 13–36.
Frith, U., Frith, C.D., 2003. Development and neurophysiology of mentalizing. Philos. Trans: Biol. Sci. 358 (1431), 459–473.
Gallagher, H.L., Frith, C.D., 2003. Functional imaging of "theory of mind.". Trends Cognit. Sci. 7 (2), 77–83.
Geraerts, E., Schooler, J.W., Merckelbach, H., Jelicic, M., Hauer, B.J.A., Ambadar, Z., 2007. The reality of recovered memories: corroborating continuous and discontinuous memories of childhood sexual abuse. Psychol. Sci. 18 (7), 564–568.
Gould, R.L., Brown, R.G., Owen, A.M., ffytche, D.H., Howard, R.J., 2003. fMRI BOLD response to increasing task difficulty during successful paired associates learning. NeuroImage 20 (2), 1006–1019.
Greicius, M.D., Krasnow, B., Reiss, A.L., Menon, V., 2003. Functional connectivity in the resting brain: a network analysis of the default mode hypothesis. Proc Natl. Acad. Sci. USA 100 (1), 253–258.
Grinband, J., Savitskaya, J., Wager, T.D., Teichert, T., Ferrera, V.P., Hirsch, J., 2011. The dorsal medial frontal cortex is sensitive to time on task, not response conflict or error likelihood. NeuroImage 57 (2), 303–311.
Hasher, L., Zacks, R.T., 1979. Automatic and effortful processes in memory. J. Exp. Psychol.: Gen. 108 (3), 356–388.
Hunter, M.A., Takane, Y., 2002. Constrained principal component analysis: various applications. J. Educ. Behav. Stat. 27 (2), 105–145.
Jersild, A.T., 1927. Mental set and shift. Arch. Psychol. 14, *89*.
Johnson, M.K., Foley, M.A., Suengas, A.G., Raye, C.L., 1988. Phenomenal characteristics of memories for perceived and imagined autobiographical events. J. Exp. Psychol. Gen. 117 (4), 371–376.
Johnson, M.K., Hashtroudi, S., Lindsay, D.S., 1993. Source monitoring. Psychol. Bull. *114* (1), 3–28.
Johnson, M.K., Kounios, J., Reeder, J.A., 1994. Time-course studies of reality monitoring and recognition. J. Exp. Psychol.: Learn., Memory, and Cogn. 20 (6), 1409–1419.
Johnson, M.K., Raye, C.L., 1981. Reality monitoring. Psychol. Rev. 88 (1), 67–85.
Kensinger, E.A., Schacter, D.L., 2006. Neural processes underlying memory attribution on a reality-monitoring task. Cerebr. Cortex 16 (8), 1126–1133, New York, N.Y.: 1991.
King, D.R., Miller, M.B., 2014. Lateral posterior parietal activity during source memory judgments of perceived and imagined events. Neuropsychologia *53*, 122–136.
Kiss, G.R., Armstrong, C., & Milroy, R. (1973). An associative thesaurus of English and its computer analysis.
Laurienti, P.J., Burdette, J.H., Wallace, M.T., Yen, Y.-F., Field, A.S., Stein, B.E., 2002. Deactivation of sensory-specific cortex by cross-modal stimuli. J. Cognit. Neurosci. 14 (3), 420–429.
Lavigne, K.M., Metzak, P.D., Woodward, T.S., 2015. Functional brain networks underlying detection and integration of disconfirmatory evidence. NeuroImage 112, 138–151.
Lavigne, K.M., Rapin, L.A., Metzak, P.D., Whitman, J.C., Jung, K., Dohen, M., Woodward, T.S., 2015. Left-dominant temporal-frontal hypercoupling in schizophrenia patients with hallucinations during speech perception. Schizophr. Bull. 41 (1), 259–267.
Leippe, M.R., Eisenstadt, D., Rauch, S.M., 2009. Cueing confidence in eyewitness identifications: influence of biased lineup instructions and pre-identification memory feedback under varying lineup conditions. Law Hum. Behav. 33 (3), 194–212.
Lindsay, D.S., 1990. Misleading suggestions can impair eyewitnesses' ability to remember event details. J. Exp. Psychol.: Learn., Mem, Cogn. 16 (6), 1077–1083.
Lindsay, D.S., Byrne, J., 2008. Source Monitoring. In: Roediger, H.L. (Ed.), Cognitive Psychology of Memory, Vol. 2. Elsevier, Oxford, pp. 325–348.
Lindsay, D.S., Johnson, M.K., 1989. The eyewitness suggestibility effect and memory for source. Mem. Cognit. 17 (3), 349–358.
Loftus, E.F., Miller, D.G., Burns, H.J., 1978. Semantic integration of verbal information into a visual memory. J. Exp. Psychol.: Hum. Learn. Mem. 4 (1), 19–31.
Mar, R.A., 2011. The neural bases of social cognition and story comprehension. Annu. Rev Psychol. 62 (1), 103–134.
McKiernan, K.A., Kaufman, J.N., Kucera-Thompson, J., Binder, J.R., 2003. A parametric manipulation of factors affecting task-induced deactivation in functional neuroimaging. J. Cogn. Neurosci. 15 (3), 394–408.
Metzak, P.D., Feredoes, E., Takane, Y., Wang, L., Weinstein, S., Cairo, T., Woodward, T. S., 2011. Constrained principal component analysis reveals functionally connected load-dependent networks involved in multiple stages of working memory. Hum. Brain Mapp. 32 (6), 856–871.
Metzak, P.D., Meier, B., Graf, P., Woodward, T.S., 2013. More than a surprise: the bivalency effect in task switching. J. Cogn. Psychol. 25 (7), 833–842.
Metzak, P.D., Riley, J.D., Wang, L., Whitman, J.C., Ngan, E.T.C., Woodward, T.S., 2012. Decreased efficiency of task-positive and task-negative networks during working memory in schizophrenia. Schizophr. Bull. 38 (4), 803–813.
Mitchell, K.J., Johnson, M.K., 2009. Source monitoring 15 years later: what have we learned from fMRI about the neural mechanisms of source memory? Psychol. Bull. 135 (4), 638–677.
Mitchell, K.J., Johnson, M.K., Raye, C.L., Greene, E.J., 2004. Prefrontal cortex activity associated with source monitoring in a working memory task. J. Cogn. Neurosci. 16 (6), 921–934.
Odinot, G., Wolters, G., Koppen, P.J. van, 2009. Eyewitness memory of a supermarket robbery: a case study of accuracy and confidence after 3 months. Law Hum. Behav. 33 (6), 506–514.
Raichle, M.E., MacLeod, A.M., Snyder, A.Z., Powers, W.J., Gusnard, D.A., Shulman, G. L., 2001. A default mode of brain function. Proc. Natl. Acad. Sci. USA 98 (2), 676–682.
Raymaekers, L., Smeets, T., Peters, M.J.V., Otgaar, H., Merckelbach, H., 2012. The classification of recovered memories: a cautionary note. Conscious. Cognit. 21 (4), 1640–1643.
Rogers, R.D., Monsell, S., 1995. Costs of a predictible switch between simple cognitive tasks. J. Exp. Psychol.: Gen. 124 (2), 207–231.
Rugg, M.D., Fletcher, P.C., Chua, P.M., Dolan, R.J., 1999. The role of the prefrontal cortex in recognition memory and memory for source: an fMRI study. NeuroImage 10 (5), 520–529.
Rugg, M.D., Vilberg, K.L., 2013. Brain networks underlying episodic memory retrieval. Current Opinion in Neurobiology *23* (2), 255–260.
Schacter, D.L., Koutstaal, W., Norman, K.A., 1996. Can cognitive neuroscience illuminate the nature of traumatic childhood memories? Curr. Opin. Neurobiol. 6 (2), 207–214.

Serences, J.T., 2004. A comparison of methods for characterizing the event-related BOLD timeseries in rapid fMRI. Neuroimage 21 (4), 1690–1700.
Simons, J.S., Owen, A.M., Fletcher, P.C., Burgess, P.W., 2005. Anterior prefrontal cortex and the recollection of contextual information. Neuropsychologia 43 (12), 1774–1783.
Slamecka, N.J., Graf, P., 1978. The generation effect: Delineation of a phenomenon. J. Exp. Psychol.: Hum. Learn Mem. 4 (6), 592–604.
Spreng, R.N., 2012. The fallacy of a "task-negative" network. Front. Psychol. 3, 145, May.
Stern, E.R., Rotello, C.M., 2000. Memory characteristics of recently imagined events and real events experienced previously. Am. J. Psychol. 113 (4), 569–590.
Subramaniam, K., Luks, T.L., Fisher, M., Simpson, G.V., Nagarajan, S., Vinogradov, S., 2012. Computerized cognitive training restores neural activity within the reality monitoring network in schizophrenia. Neuron 73 (4), 842–853.
Takane, Y., Hunter, M.A., 2001. Constrained principal component analysis: a comprehensive theory. Appl. Algebra Eng., Commun. Comput. 12 (5), 391–419.
Takane, Y., Shibayama, T., 1991. Principal component analysis with external information on both subjects and variables. Psychometrika 56 (1), 97–120.
Vincent, J.L., Snyder, A.Z., Fox, M.D., Shannon, B.J., Andrews, J.R., Raichle, M.E., Buckner, R.L., 2006. Coherent spontaneous activity identifies a hippocampal-parietal memory network. J. Neurophysiol. 96 (6), 3517–3531.
Vinogradov, S., Luks, T.L., Schulman, B.J., Simpson, G.V., 2008. Deficit in a neural correlate of reality monitoring in schizophrenia patients. Cerebr. Cortex 18 (11), 2532–2539.
Vinogradov, S., Luks, T.L., Simpson, G.V., Schulman, B.J., Glenn, S., Wong, A.E., 2006. Brain activation patterns during memory of cognitive agency. Neuroimage 31 (2), 896–905.
Wagner, A.D., Shannon, B.J., Kahn, I., Buckner, R.L., 2005. Parietal lobe contributions to episodic memory retrieval. Trends Cognit. Sci. 9 (9), 445–453.
Williams, J.H.G., 2008. Self-other relations in social development and autism: multiple roles for mirror neurons and other brain bases. Autism Res. : Off. J. Int. Soc. Autism Res. 1 (2), 73–90.
Woodward, T.S., Feredoes, E., Metzak, P.D., Takane, Y., Manoach, D.S., 2013. Epoch-specific functional networks involved in working memory. NeuroImage 65, 529–539.
Woodward, T.S., Menon, M., Whitman, J.C., 2007. Source monitoring biases and auditory hallucinations. Cogn. Neuropsychiatry 12 (6), 477–494.
Woodward, T.S., Metzak, P.D., Meier, B., Holroyd, C.B., 2008. Anterior cingulate cortex signals the requirement to break inertia when switching tasks: a study of the bivalency effect. NeuroImage 40 (3), 1311–1318.
Woodward, T.S., Ruff, C.C., Ngan, E.T.C., 2006. Short- and long-term changes in anterior cingulate activation during resolution of task-set competition. Brain Res. 1068 (1), 161–169.
Yeo, B.T.T., Krienen, F.M., Sepulcre, J., Sabuncu, M.R., Lashkari, D., Hollinshead, M., Buckner, R.L., 2011. The organization of the human cerebral cortex estimated by intrinsic functional connectivity. J. Neurophysiol. 106 (3), 1125–1165.
Yonelinas, A.P., 2002. The nature of recollection and familiarity: a review of 30 years of research. J. Mem. Lang. 46, 441–517.